# UC Irvine
## UC Irvine Previously Published Works

**Title**

Eliminating microglia in Alzheimer's mice prevents neuronal loss without modulating amyloid-β pathology.

**Permalink**

https://escholarship.org/uc/item/1dk665b9

**Journal**

Brain : a journal of neurology, 139(Pt 4)

**ISSN**

0006-8950

**Authors**

Spangenberg, Elizabeth E
Lee, Rafael J
Najafi, Allison R
et al.

**Publication Date**

2016-04-01

**DOI**

10.1093/brain/aww016

Peer reviewed

# BRAIN
A JOURNAL OF NEUROLOGY

# Eliminating microglia in Alzheimer's mice prevents neuronal loss without modulating amyloid-β pathology

Elizabeth E. Spangenberg,[1] Rafael J. Lee,[1] Allison R. Najafi,[1] Rachel A. Rice,[1] Monica R. P. Elmore,[1] Mathew Blurton-Jones,[1] Brian L. West[2] and Kim N. Green[1]

In addition to amyloid-β plaque and tau neurofibrillary tangle deposition, neuroinflammation is considered a key feature of Alzheimer's disease pathology. Inflammation in Alzheimer's disease is characterized by the presence of reactive astrocytes and activated microglia surrounding amyloid plaques, implicating their role in disease pathogenesis. Microglia in the healthy adult mouse depend on colony-stimulating factor 1 receptor (CSF1R) signalling for survival, and pharmacological inhibition of this receptor results in rapid elimination of nearly all of the microglia in the central nervous system. In this study, we set out to determine if chronically activated microglia in the Alzheimer's disease brain are also dependent on CSF1R signalling, and if so, how these cells contribute to disease pathogenesis. Ten-month-old 5xfAD mice were treated with a selective CSF1R inhibitor for 1 month, resulting in the elimination of ~80% of microglia. Chronic microglial elimination does not alter amyloid-β levels or plaque load; however, it does rescue dendritic spine loss and prevent neuronal loss in 5xfAD mice, as well as reduce overall neuroinflammation. Importantly, behavioural testing revealed improvements in contextual memory. Collectively, these results demonstrate that microglia contribute to neuronal loss, as well as memory impairments in 5xfAD mice, but do not mediate or protect from amyloid pathology.

1 Department of Neurobiology and Behavior, Institute for Memory Impairments and Neurological Disorders, University of California, Irvine, CA, 92697-4545, USA
2 Plexxikon Inc., Berkeley, California, 94710, USA

Correspondence to: Kim N. Green, Ph.D.,
3208 Biological Sciences III,
University of California, Irvine,
Irvine, CA 92697-4545, USA
E-mail: kngreen@uci.edu

**Keywords:** microglia; Alzheimer's disease; amyloid; inflammation; cognition

## Introduction

Alzheimer's disease is a progressive neurodegenerative disease classically characterized by the presence of amyloid plaques and neurofibrillary tangles. However, histological studies demonstrate that neuroinflammation is also a key feature of the Alzheimer's disease brain (Fillit *et al.*, 1991; Ishizuka *et al.*, 1997; McGeer and McGeer, 1999; Cagnin *et al.*, 2001; Dandrea *et al.*, 2001), as well as being prominently observed in amyloid precursor protein (APP) overexpressing transgenic mouse models (Kitazawa *et al.*, 2005). These studies show that activated microglia surround extracellular plaques (Rozemuller *et al.*, 1986; Dickson *et al.*, 1988; Mattiace *et al.*, 1990), likely in an attempt to clear the toxic deposits, and stain positively for inflammatory markers, including major histocompatibility complex (MHC) class II,

cyclooxygenase 2, tumor necrosis factor α (*TNFA*), interleukin-1β (*IL1B*), and IL16 (Akiyama *et al.*, 2000). Inevitably, the sustained activation of microglia results in a chronic neuroinflammatory response and the increased production of pro-inflammatory cytokines, such as TNF-α and IL-1β (Meda *et al.*, 1995; Akama and Van Eldik, 2000; Cacquevel *et al.*, 2004). Previous investigations indicate that this chronic neuroinflammation response is synaptotoxic and neurotoxic (Hauss-Wegrzyniak *et al.*, 2002; Centonze *et al.*, 2009; Ziehn *et al.*, 2010) and exacerbates cognitive decline (Kitazawa *et al.*, 2011). Indeed, mouse models of Alzheimer's disease display striking dendritic spine loss that is spatially associated with these microglia-surrounded plaques (Dong *et al.*, 2007; Grutzendler and Gan, 2007; Spires-Jones *et al.*, 2007). In humans, studies have identified synaptic loss as a correlate of, and a major contributor to, cognitive decline (Scheff *et al.*, 2006; Robinson *et al.*, 2014). Of relevance, recent genome-wide association studies have uncovered several risk-associated genes in the development of sporadic Alzheimer's disease (Medway and Morgan, 2014). Most of these risk genes are either expressed by microglia or associated with their reactivity, including *CD2AP* (Srivatsan *et al.*, 2013), *CD33* (Bradshaw *et al.*, 2013), *BIN1* (Butovsky *et al.*, 2014), *CR1* (Crehan *et al.*, 2013), *PICALM* (Ando *et al.*, 2013), *ABCA7* (Kim *et al.*, 2013), *TREM2* (Guerreiro *et al.*, 2013), and *CLU* (Xu *et al.*, 2000). Thus, genetic changes in microglia-associated genes correspond strongly with an increased risk of developing Alzheimer's disease. For these reasons, we hypothesized that microglia play a critical role in the development and progression of Alzheimer's disease by limiting amyloid-β/plaque loads, but contribute to synaptic and neuronal loss.

We have previously shown that microglia in the adult brain are fully dependent on CSF1R signalling for their survival (Elmore *et al.*, 2014). Administration of CSF1R inhibitors that cross the blood–brain barrier lead to brain-wide elimination of ~80% of all microglia within 7 days of treatment. Moreover, these microglia remain eliminated for the duration of treatment, even for weeks or months. As microglia are the only cell type to express CSF1R in the adult brain parenchyma, the effects of this treatment are largely restricted to this cellular compartment. Of note, peripheral myeloid populations are also known to express CSF1R, but those explored thus far are not dramatically eliminated by the doses and compounds used in this study (Chitu *et al.*, 2012; Elmore *et al.*, 2014; Kim *et al.*, 2014; Mok *et al.*, 2014; Valdearcos *et al.*, 2014), although their functions/response to disease may be altered due to inhibition.

In this study, we set out to show that microglia in the Alzheimer's disease brain are also dependent on CSF1R signalling and to explore the effects of chronic microglial elimination on Alzheimer's disease pathologies and memory in 5xfAD mice. The 5xfAD mice represent an aggressive model of amyloid pathologies, with amyloid-β plaques first depositing from 2 months of age (Oakley *et al.*, 2006). Notably, 5xfAD mice exhibit marked synaptic and neuronal loss as pathology develops, with neuronal loss

seen in the subiculum from 10 months of age (Jawhar *et al.*, 2012; Buskila *et al.*, 2013; Eimer and Vassar, 2013; Crowe and Ellis-Davies, 2014), allowing for investigations into how the pathology drives damage to neurons and neuronal structures. Through the elimination of microglia in advanced pathology 5xfAD mice, we show recovery of contextual memory, a reversal of dendritic spine loss and prevention of neuronal loss, yet no changes on amyloid-β levels or plaque loads, highlighting the roles that microglia may play in the Alzheimer's disease brain.

# Materials and methods

## Compounds

PLX3397 was provided by Plexxikon Inc. and formulated in AIN-76A standard chow by Research Diets Inc. at 290 mg/kg or 600 mg/kg, as previously described (Elmore *et al.*, 2014). PLX5622 was provided by Plexxikon Inc. and formulated in AIN-76A standard chow by Research Diets Inc. at 1200 mg/kg.

## Animal treatments

All rodent experiments were performed in accordance with animal protocols approved by the Institutional Animal Care and Use Committee at the University of California, Irvine. CSF1R-iCRE [FVB-Tg(Csf1r-icre)1Jwp/J] and *Rosa26*[YFP] (B6.129X1-Gt(ROSA)26Sor[tm1(EYFP)Cos]/J) reporter mice were obtained from The Jackson Laboratory. Crossing these mice yielded CSF1R-iCRE/Rosa26YFP progeny that express yellow fluorescent protein (YFP) in all cells that either transiently or constitutively express CSF1R, which in the brain predominantly labels microglia. Two-month-old mice were treated for 7 days with PLX3397 (600 mg/kg in chow) to eliminate microglia. The 5xfAD mouse model has been previously described in detail (Oakley *et al.*, 2006). Using a 2 × 2 factorial design, forty male and female 10-month-old wild-type (C57BL/6 background) or 5xfAD mice were treated with either PLX3397 for 28 days to eliminate microglia or control chow, creating four treatment groups (*n* = 10/group): Control (six males and four females), PLX3397 (six males and four females), 5xfAD (four males and six females), and 5xfAD + PLX3397 (four males and six females). At this age, 5xfAD mice display extensive pathology, synaptic loss, and neuronal loss (Oakley *et al.*, 2006; Buskila *et al.*, 2013; Eimer and Vassar, 2013). After 28 days of treatment, behavioural testing commenced while animals remained on their respective diets. A second cohort of 14-month-old 5xfAD mice (*n* = 4/group; 5xfAD = four males, and 5xfAD + PLX5622 = three males and one female) was treated with either PLX5622 for 28 days to deplete microglia or control chow (5xfAD versus 5xfAD + PLX5622). A third cohort of 1.5-month-old 5xfAD mice (*n* = 4/group; two males and two females) was treated with PLX3397 or control for 28 days (5xfAD versus 5xfAD + PLX3397). Following behavioural testing in the 10-month-old cohort, and following inhibitor treatment in the 14-month-old and 1.5-month-old cohorts, mice were euthanized via $CO_2$ inhalation and transcardially perfused with phosphate-buffered saline. For both studies, brains were removed

and hemispheres separated along the midline. Brain halves were either flash frozen for subsequent biochemical analysis, drop-fixed in 4% paraformaldehyde (Thermo Fisher Scientific) for subsequent immunohistochemical analysis, or placed in Golgi impregnation solution for subsequent dendritic spine analysis. Fixed half brains were sliced at 40 μm using a Leica SM2000 R freezing microtome. The flash-frozen hemispheres were ground with a mortar and pestle to yield a fine powder. One-half of the powder was homogenized in Tissue Protein Extraction Reagent, T-PER (Life Technologies) with protease (Roche) and phosphatase inhibitors (Sigma-Aldrich). The second half was processed with an RNA Plus Universal Mini Kit (Qiagen) for RNA analysis.

## Behavioural testing

Behaviour was analysed 28 days after the administration of PLX3397 treatment to eliminate microglia. Methods for testing mice on contextual fear conditioning were based on previous literature (Rodriguez-Ortiz *et al.*, 2013; Elmore *et al.*, 2014). To assess contextual memory, freezing behaviour, defined as the total lack of body movement except for respiration, was scored live and video-recorded. Behaviour was scored using 1-0 sampling every 10 s, with a 1 denoting positive freezing behaviour and 0 indicating the absence of freezing behaviour. For the training trial, mice were placed in a fear-conditioning chamber (Gemini, San Diego Instruments; 24.1-cm length × 20.3-cm width × 20.3-cm height) and allowed to explore for 2 min before receiving one foot shock (3 s, 0.2 mA). Animals were returned to their home cage 30 s after the shock. Testing was conducted 24 h later, in which the animals were placed in the chamber and allowed to explore for 5 min.

## Confocal microscopy

Immunofluorescent labelling was performed following a standard indirect technique as previously described (Neely *et al.*, 2011). Primary antibodies and dilutions used are as follows: anti-ionized calcium-binding adapter molecule 1 (IBA1; 1:1000; Wako), anti-amyloid-$\beta_{1-16}$ (6E10; 1:1000; Covance), anti-s100β (1:200; Abcam), anti-aldehyde dehydrogenase family 1 member L1 (Aldh1L1; 1:50; UC Davis), and anti-glial fibrillary protein (GFAP; 1:1000; Abcam). Thioflavin-S (Sigma-Aldrich) staining was carried out as previously described (Rice *et al.*, 2014). Total microglia and plaque counts were obtained by imaging comparable sections of tissue from each animal at the 10× objective, followed by automated analyses using Bitplane Imaris 7.5 spots or surfaces modules, respectively. To determine the number of plaque-associated microglia, equal perimeters were drawn around each plaque using ImageJ software (NIH), and cells were manually counted.

## Immunoblotting

Immunoblotting was performed as previously described (Elmore *et al.*, 2014). Antibodies and dilutions used in this study include: 6E10 (as described above), CT20 (1:1000; Calbiochem) for C99 and C83, and β-actin (1:10 000; Sigma-Aldrich). Quantitative densitometric analyses were performed on digitized images of immunoblots with ImageJ software.

## Amyloid-β enzyme-linked immuno-sorbent assay

Isolated protein samples were transferred to a blocked MSD Human/Rodent (4G8) amyloid-β triplex ELISA plate (amyloid-$\beta_{1-38}$, amyloid-$\beta_{1-40}$, amyloid-$\beta_{1-42}$) and incubated for 2 h at room temperature with an orbital shaker. The plate was then washed and measurements obtained using a SECTOR Imager 2400, according to the manufacturer's instructions (Meso Scale Discovery).

## NanoString RNA analysis

One hundred and eighty inflammation-, Alzheimer's disease-, plasticity-, and ageing-related genes were selected for analysis and probes were designed and synthesized by NanoString nCounter™ technologies (NanoString) against mouse genes. Total mRNA was extracted using an RNA Plus Universal Mini Kit (Qiagen) and was hybridized and multiplexed with NanoString probes, according to the manufacturer's instructions. Counts for target genes were normalized to house-keeping genes (*Eef1g*, *G6pdx*, *Hprt*, *Polr1b*, *Polr2a*, *Ppia*, *Rpl19*, *Sdha*, and *Tbp*) to account for variability in the RNA content. Background signal was calculated as a mean value of the negative hybridization control probes. Normalized counts were log-transformed for downstream statistical analysis.

## Golgi staining and spine quantification

Half brains were sliced coronally with a vibratome at 100 μm, mounted on gelatin-coated slides, and subsequently stained using a SuperGolgi Kit, per the manufacturer's instructions (Bienno Tech). Five non-primary apical dendrites in the CA1 per animal (*n* = 3/group) were traced using a 100× oil-immersion objective and Neurolucida software for dendritic spine analysis (MBF Bioscience). Spines were classified based on previous literature using head-to-neck ratios and quantified according to the following categories: total, mushroom, stubby, and thin spines (Peters and Kaiserman-Abramof, 1970).

## Cresyl violet staining and neuron quantification

Cresyl violet staining was performed on fixed tissue and neurons in the subiculum were counted in a double-blind unbiased stereological fashion, as previously described (Myczek *et al.*, 2014). All unbiased stereological assessments were performed using Stereo Investigator (MBF Bioscience) and Neurolucida softwares. The stereological quantification of neurons in the subiculum was performed on every sixth section (40 μm coronal sections between −2.48 mm and −3.28 mm posterior to bregma) of one brain hemisphere (*n* = 4/group). A counting frame of 50 × 50 μm in a sampling grid of 100 × 100 μm was used, with a guard zone height of 3 μm for the top and bottom. The subiculum was defined using a 5× objective and the Cresyl violet stained cells were counted using a 100× oil-immersion objective. Neuronal nuclei were randomly sampled from the defined subiculum using the optical dissector probes.

## Statistics

Behavioural, biochemical, and immunohistological data were analysed using either unpaired Student's *t*-test (Control versus wild-type or 5xfAD versus 5xfAD + PLX3397/PLX5622) in Microsoft Excel or as a two-way ANOVA (Diet: Control versus PLX3397 and Genotype: wild-type versus 5xfAD) using the MIXED procedure of the Statistical Analysis Systems software (SAS Institute Inc.), a general linear model that accounts for both fixed and random variables, as previously described (Elmore *et al.*, 2015). *Post hoc* paired contrasts were used to examine biologically relevant interactions from the two-way ANOVA regardless of statistical significance of the interaction. Symbols denote significant differences between groups ($P < 0.05$): *Control versus PLX3397; [†]Control versus 5xfAD; [#]PLX3397 versus 5xfAD + PLX3397; [φ]5xfAD versus 5xfAD + PLX3397. Data are presented as raw means ± standard error of the mean (SEM). For all analyses, statistical significance was accepted at $P < 0.05$ (*) and trends at $P < 0.10$ ([#]).

# Results

## CSF1R inhibition eliminates microglia

PLX3397 is an orally bioavailable selective CSF1R/c-kit inhibitor that crosses the blood–brain barrier (Elmore *et al.*, 2014), which has shown recent clinical efficacy at reducing tumour size in pigmented villonodular synovitis (Tap *et al.*, 2015) and previously, we have reported that CSF1R inhibition results in the elimination of microglia (Elmore *et al.*, 2014). To address the possibility that microglia are downregulating myeloid/microglial genes with treatment, we crossed CSF1R-iCRE mice with *Rosa26*[YFP] reporter mice to generate offspring that express YFP in all CSF1R expressing cells under control of the Rosa26 locus (Fig. 1A). As such, these mice express YFP in all microglial progeny, as well as any potential cells that have differentiated from microglia. Accordingly, immunolabelling for microglia with IBA1 and YFP indicates that the expression of YFP is restricted to the microglial compartment (Fig. 1B), and that both IBA1^{+} and YFP^{+} cells are eliminated with PLX3397 treatment. Quantification of YFP and IBA1 expression revealed an ∼88% and ∼99% reduction in cell number with PLX3397-treatment, respectively (Fig. 1C). This conclusively demonstrates that treatment with the CSF1R inhibitor PLX3397 eliminates microglia in the adult mouse brain, rather than simply causing a transient loss of microglial signature.

## CSF1R inhibition improves contextual memory deficits in 5xfAD mice following microglial elimination

Ten-month-old 5xfAD mice were selected for this study as they show extensive amyloid pathology at this age, along with robust neuroinflammation and also synaptic loss, mimicking the human condition. Crucially, these mice begin to exhibit neuronal loss from 10 months of age. Following 28 days of PLX3397 or control chow treatment, 5xfAD and wild-type mice were tested in contextual fear conditioning to assess hippocampal memory (see experimental schematic; Fig. 2A). Analysis of behavioural performance revealed that 5xfAD mice spent significantly less time freezing compared to controls, but this effect trended toward recovery in 5xfAD mice administered PLX3397 to eliminate microglia ($P = 0.0813$; Fig. 2B).

Following behavioural testing, the brains of these mice were analysed for Thioflavin-S staining and IBA1 immunolabelling to visualize dense core plaques and microglia, respectively (Fig. 2C and D). 5xfAD mice had significantly elevated total numbers of IBA1^{+} cells, but these were reduced by ∼80% in the hippocampus, cortex, and thalamus of PLX3397-treated animals (Fig. 2E), revealing the majority of these cells to be dependent on CSF1R signalling for their survival, particularly in the intra-plaque spaces. High power *z*-stack images showed microglia to be highly associated with dense core plaques in these mice (Fig. 2F). Importantly, PLX3397 treatment was able to significantly reduce these plaque-associated microglia by ∼50% (Fig. 2G). Quantification of the number of non-plaque associated IBA1^{+} cells revealed a ∼90% reduction in the treated 5xfAD mice (Fig. 2H), highlighting the preferential elimination of non-plaque associated IBA1^{+} cells. Combined, these findings indicate that microglia in 5xfAD mice may be involved in mediating contextual memory deficits, which can be partially attenuated by eliminating the microglial compartment.

## Microglia do not modulate amyloid-β pathology

To determine if microglia mediate amyloid pathology, we examined the effects of eliminating microglia on amyloid-β levels in the brain. Staining for dense-core plaques via Thioflavin-S showed that microglial depletion did not significantly affect plaque numbers or average plaque size in any brain region analysed (Fig. 3A–D). Plaques were categorized by size (i.e. $< 150 \ \mu m^2$, $150–1000 \ \mu m^2$, or $> 1000 \ \mu m^2$) in the thalamus, due to high plaque load observed in this region (Fig. 3A–D), but no differences were found between control- and PLX3397-treated mice (Fig. 3E). We then analysed both soluble and insoluble levels of amyloid-$\beta_{1–38}$, amyloid-$\beta_{1–40}$, and amyloid-$\beta_{1–42}$ by triplex ELISA. In wild-type mice, there was no effect of microglial elimination on levels of endogenous amyloid-β species (Fig. 3F), whereas amyloid-$\beta_{1–38}$ was below detection limits. We also found no significant differences in amyloid-β levels in either soluble or insoluble fractions in 5xfAD mice (Fig. 3G and H). Finally, we immunolabelled tissue with 6E10 antibody, to assess the effect of PLX3397 treatment on diffuse plaque load and quantified the size of plaques
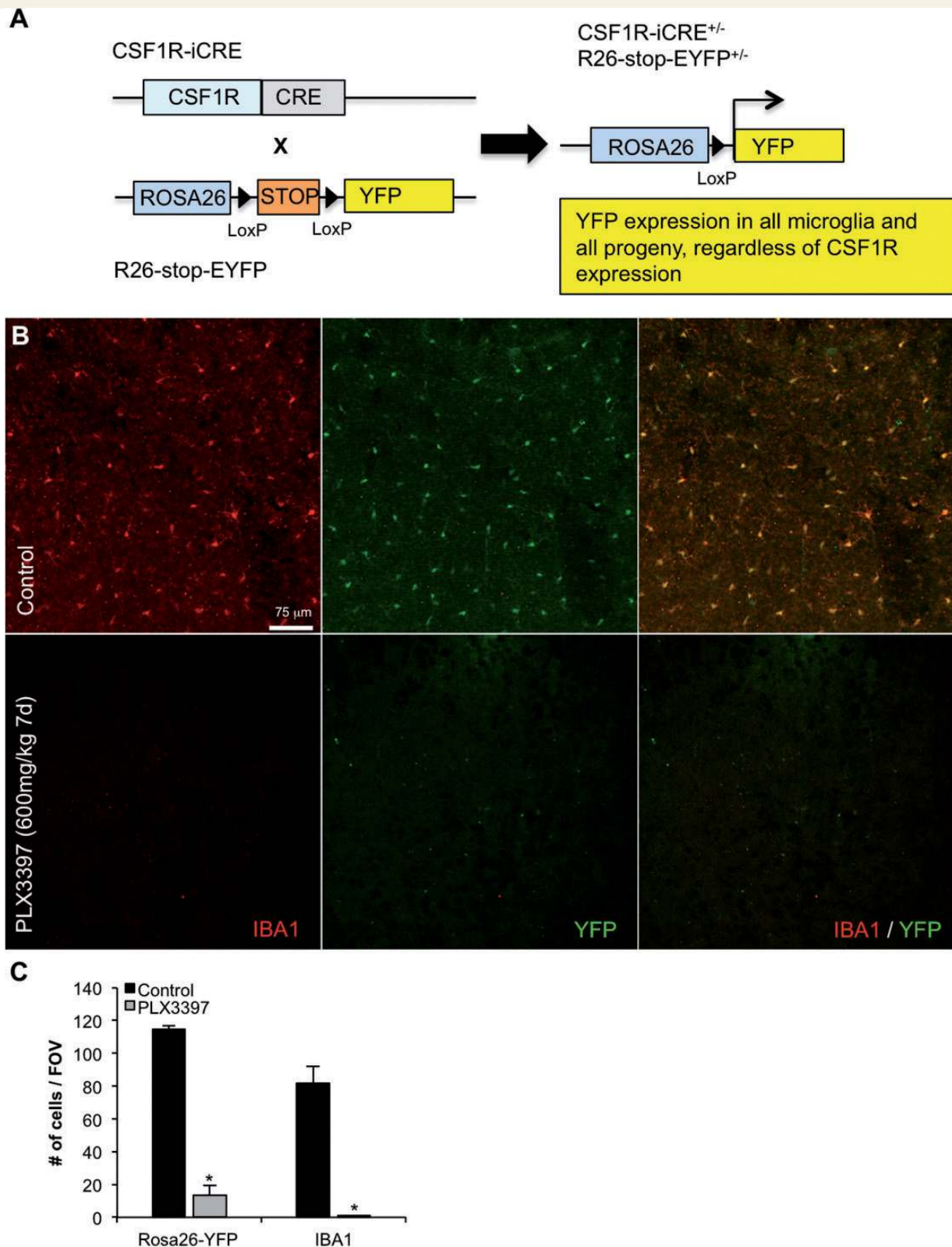
**Figure 1  Treatment with the CSF1R inhibitor PLX3397 eliminates microglia in Rosa26-YFP mice.** Two-month-old mice were treated with PLX3397 (600 mg/kg) for 7 days to eliminate microglia. (**A**) Schematic of the breeding strategy to yield offspring with YFP expressing microglia. (**B**) Immunolabelling for microglia (IBA1 in red) and expression of YFP in CSF1R^{+}/derived cells (YFP in green). (**C**) Quantification of the number of YFP[+] and IBA1^{+} cells is reduced in the cortex by 88% ($P < 0.0001$) and 99% ($P < 0.0001$), respectively, with PLX3397 treatment. Statistical significance is denoted by [*]$P < 0.05$. Error bars indicate SEM ($n = 4$/group).
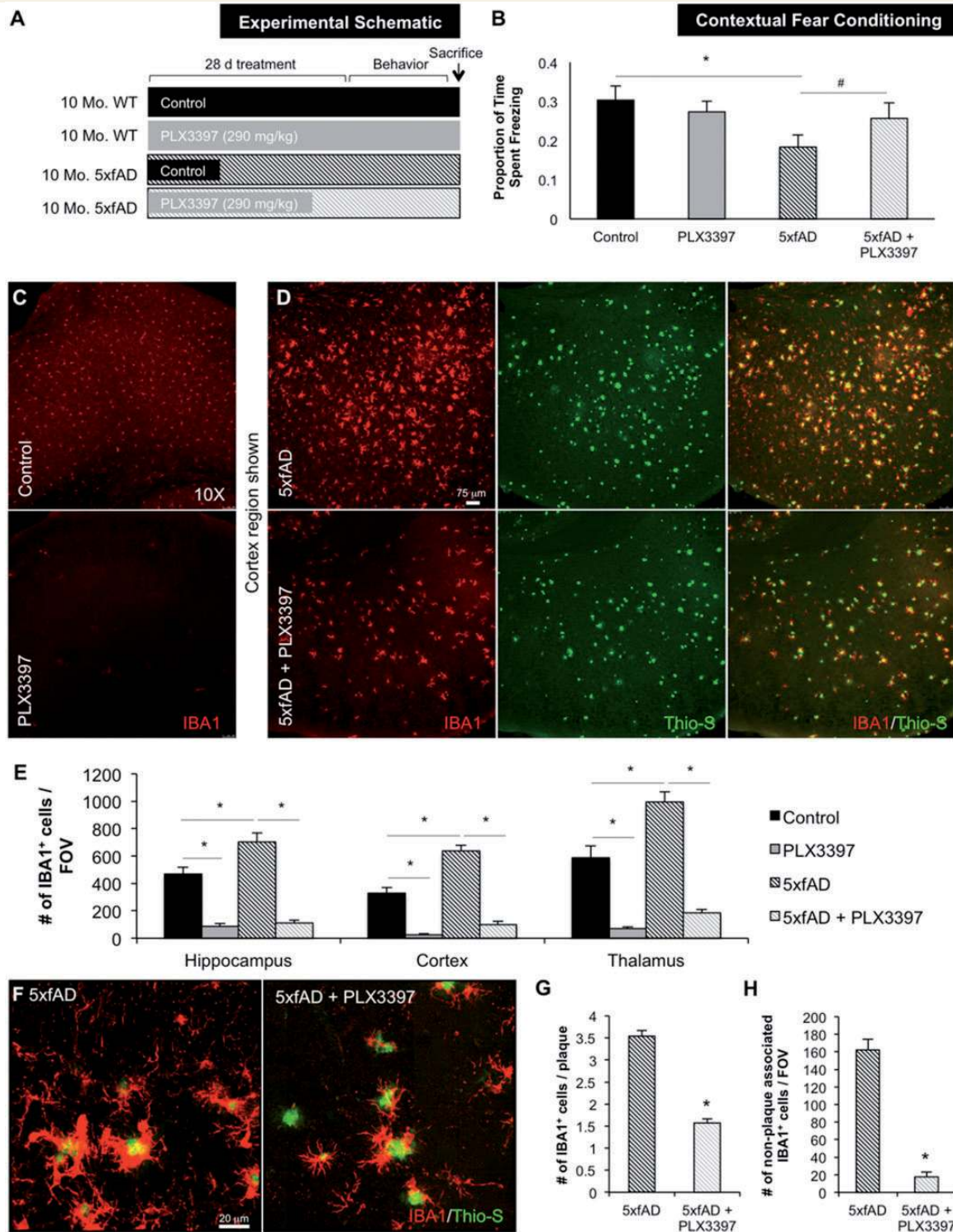
**Figure 2 Chronically activated microglia in 5xfAD mice are dependent on CSF1R signalling for their survival.** Ten-month-old wild-type or 5xfAD mice were treated with control chow or PLX3397 for 28 days to eliminate microglia. (**A**) Experimental design. (**B**) In contextual fear conditioning, 5xfAD mice spent significantly less time freezing compared to control (via two-way ANOVA, $P = 0.0196$) and 5xfAD + PLX3397 treated mice trended to an increased freezing time (via two-way ANOVA, $P = 0.0813$). (**C** and **D**) Immunolabelling for microglia (IBA1 in red) and staining for dense-core plaques (Thio-S in green). (**E**) Microglia number is increased by ~40% in 5xfAD mice compared to control (via two-way ANOVA, $P < 0.0001$). PLX3397 treatment eliminates ~80% of microglia in both wild-type and 5xfAD mice (via two-way ANOVA, $P < 0.001$). (**F**) Representative 63X IBA1 Thio-S immunofluorescent staining of the cortex. (**G**) Quantification of plaque-associated microglia reveals the number of these cells was reduced by ~50% with PLX3397 treatment (two-tailed unpaired *t*-test, $P < 0.0001$). (**H**) The number of non-plaque associated microglia is reduced by ~90% with PLX3397 treatment in 5xfAD mice (two-tailed unpaired *t*-test, $P < 0.0001$). Statistical significance is denoted by $^*P < 0.05$ and statistical trends by $^\#P < 0.10$. Error bars indicate SEM ($n = 7$/group).
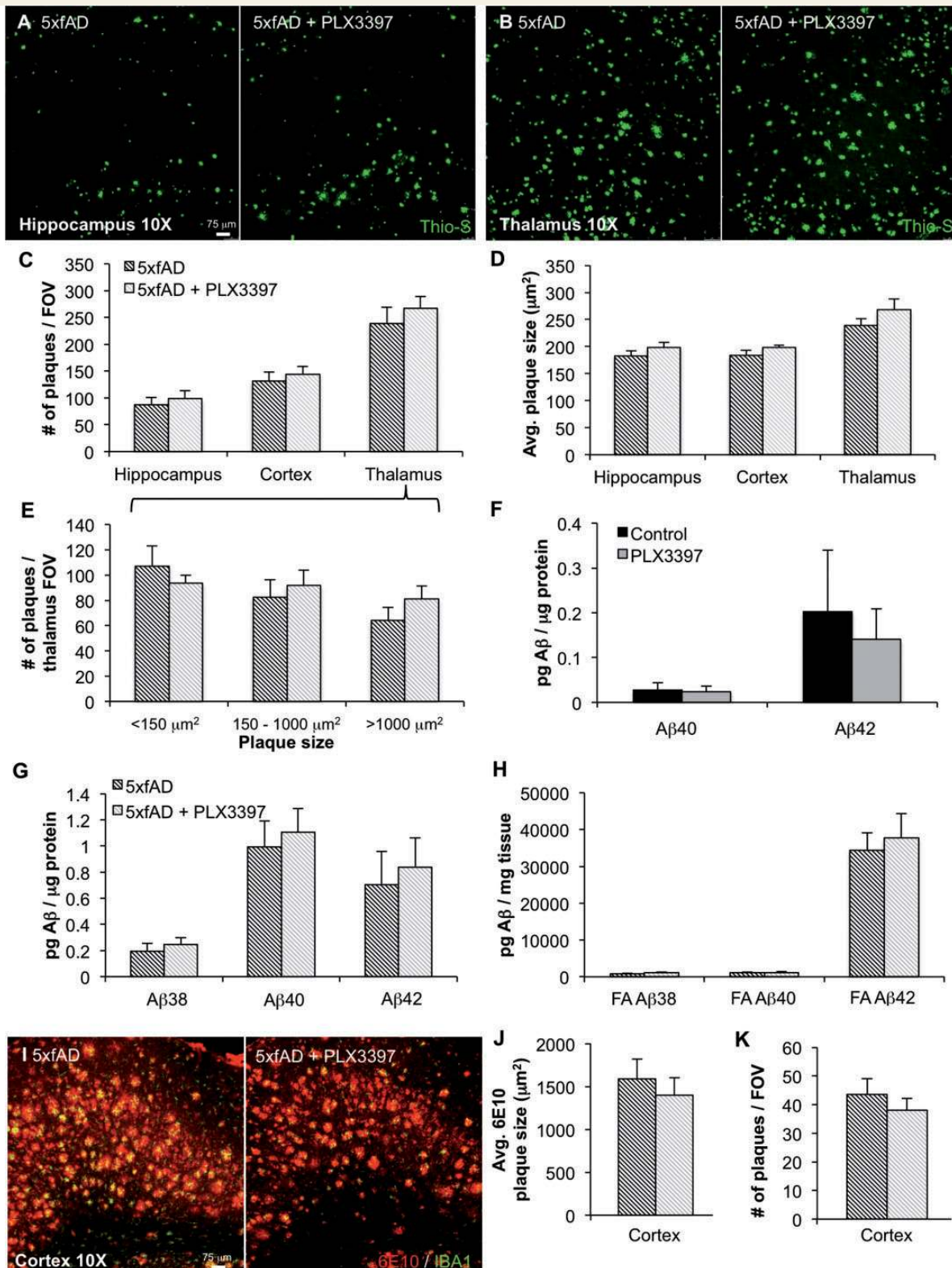
**Figure 3 Elimination of microglia does not modulate amyloid-β levels or plaque load.** (**A** and **B**) Representative hippocampal and thalamic $10\times$ images of dense core plaques (Thio-S) in 5xfAD and 5xfAD mice treated with PLX3397. (**C** and **D**) Quantification of number of Thio-S$^+$ plaques and average area of the plaques in the hippocampus, cortex, and thalamus. (**E**) Microglial elimination has no effect on plaques of any size. (**F**) Levels of amyloid-$\beta_{1-40}$ and amyloid-$\beta_{1-42}$ were unchanged with microglial elimination in wild-type mice. Levels of amyloid-$\beta_{1-38}$ were below detection threshold. (**G**). (**H**) Levels of amyloid-β species in detergent-soluble and formic acid-soluble (FA) fractions are not changed with microglial elimination. (**I**) Representative $10\times$ 6E10 and IBA1 immunofluorescent images of the thalamus. (**J** and **K**) Quantification of 6E10$^+$ plaque size and numbers reveals no effect of microglial elimination. Error bars indicate SEM ($n = 7$/group).
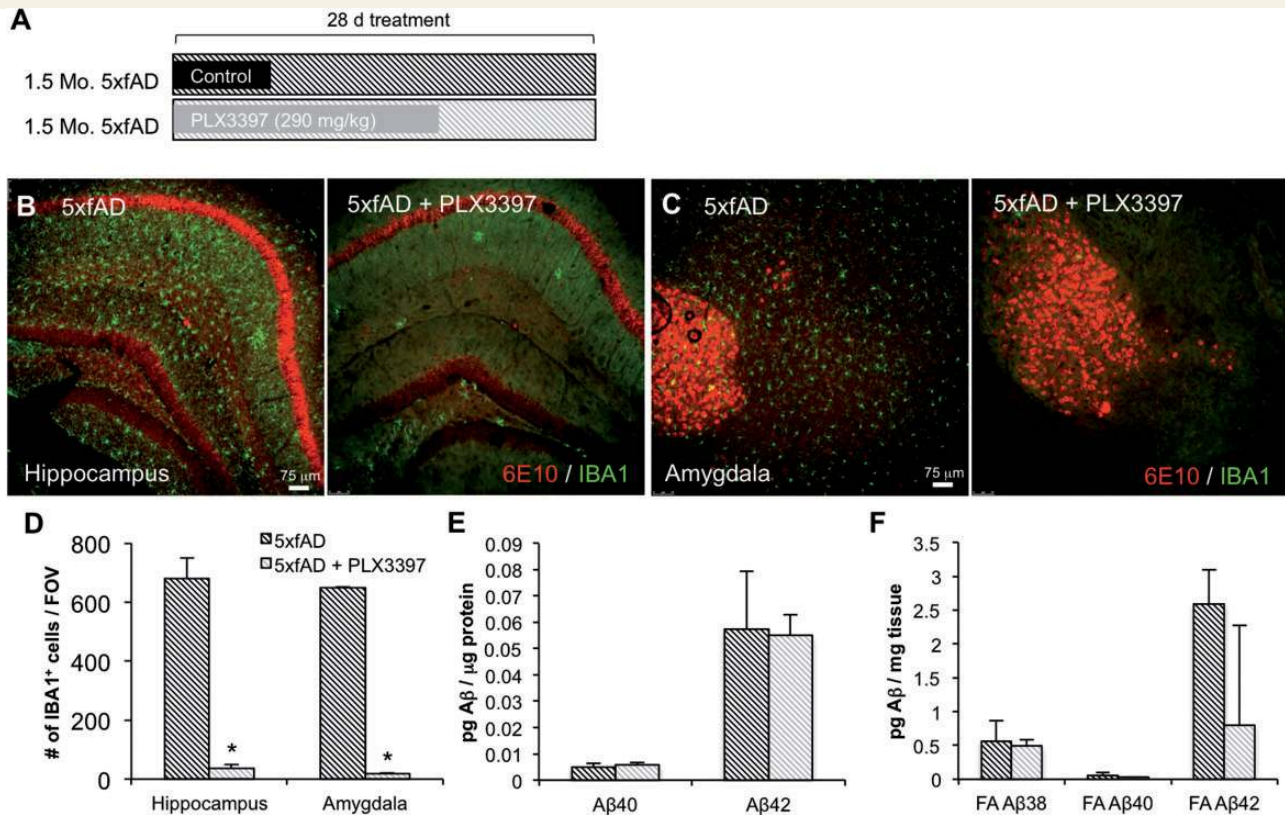
**Figure 4 Microglial elimination in young 5xfAD mice does not affect amyloid-β pathology.** One and a half-month-old 5xfAD mice were treated with PLX3397 or control chow for 28 days. (**A**) Experimental design. (**B** and **C**) Representative $10\times$ immunofluorescent IBA1 and 6E10 images of the hippocampus and amygdala. (**D**) Quantification of microglial cells shows a significant reduction in the 5xfAD + PLX3397 group compared to the 5xfAD group in the hippocampus and amygdala (two-tailed unpaired $t$-test, $P < 0.0001$). (**E** and **F**) Levels of amyloid-β species in detergent-soluble fractions are unchanged with the elimination of microglia. Levels of amyloid-$\beta_{1-38}$ in the detergent-soluble fraction were below detection threshold. Statistical significance is denoted by $^{*}P < 0.05$. Error bars indicate SEM ($n = 4$/group). FOV = field of view.

(Fig. 3I). In the cortex, we found no differences in diffuse plaque load or size with PLX3397 treatment (Fig. 3J and K). Collectively, these data indicate that microglia do not play a substantial role in amyloid-β production/clearance or plaque deposition/remodelling in pathological 5xfAD mice.

## Elimination of microglia in young 5xfAD mice reveals no changes in amyloid-β pathology

Given the surprising result that elimination of microglia did not affect amyloid-β load or levels in pathological 5xfAD mice, we sought to determine if microglia were protective at younger ages or in the absence of pathology. As 5xfAD mice develop plaques from ~2 months of age, we treated 1.5-month-old mice with PLX3397 for 28 days (Fig. 4A). Immunolabelling for IBA1 and 6E10 (Fig. 4B and C) revealed extensive intraneuronal 6E10 reactivity in CA1 and amygdala neurons in both groups, but no extracellular plaques were observed. Microglial counts in these regions showed a ~95% decrease with PLX3397 treatment (Fig. 4D). To analyse amyloid-β, we used triplex ELISA to

assess protein levels of amyloid-$\beta_{1-38}$, amyloid-$\beta_{1-40}$, and amyloid-$\beta_{1-42}$. We found no effect of microglial elimination on the amount of soluble (Fig. 4E) or insoluble (Fig. 4F) amyloid-β protein. Together, these data indicate that microglia do not protect against amyloid-β accumulation in the 5xfAD mice at a pre-plaque age.

## Elimination of microglia in aged 5xfAD mice with the specific CSF1R inhibitor PLX5622

PLX5622 is a brain-penetrant inhibitor of CSF1R that quickly eliminates microglia, but does not inhibit c-kit (Valdearcos *et al.*, 2014; Dagher *et al.*, 2015). To confirm the effects of PLX3397 and to rule out other off-target effects, we treated a second cohort of 5xfAD mice for 28 days with 1200 mg/kg PLX5622 in chow. We again stained tissue for dense core plaques using Thioflavin-S and immunolabelled microglia with IBA1 (Fig. 5A). Microglia were dramatically depleted with treatment, with most of the remaining cells being associated with dense core plaques, as with PLX3397 treatment (Fig. 5B and E). Quantification revealed
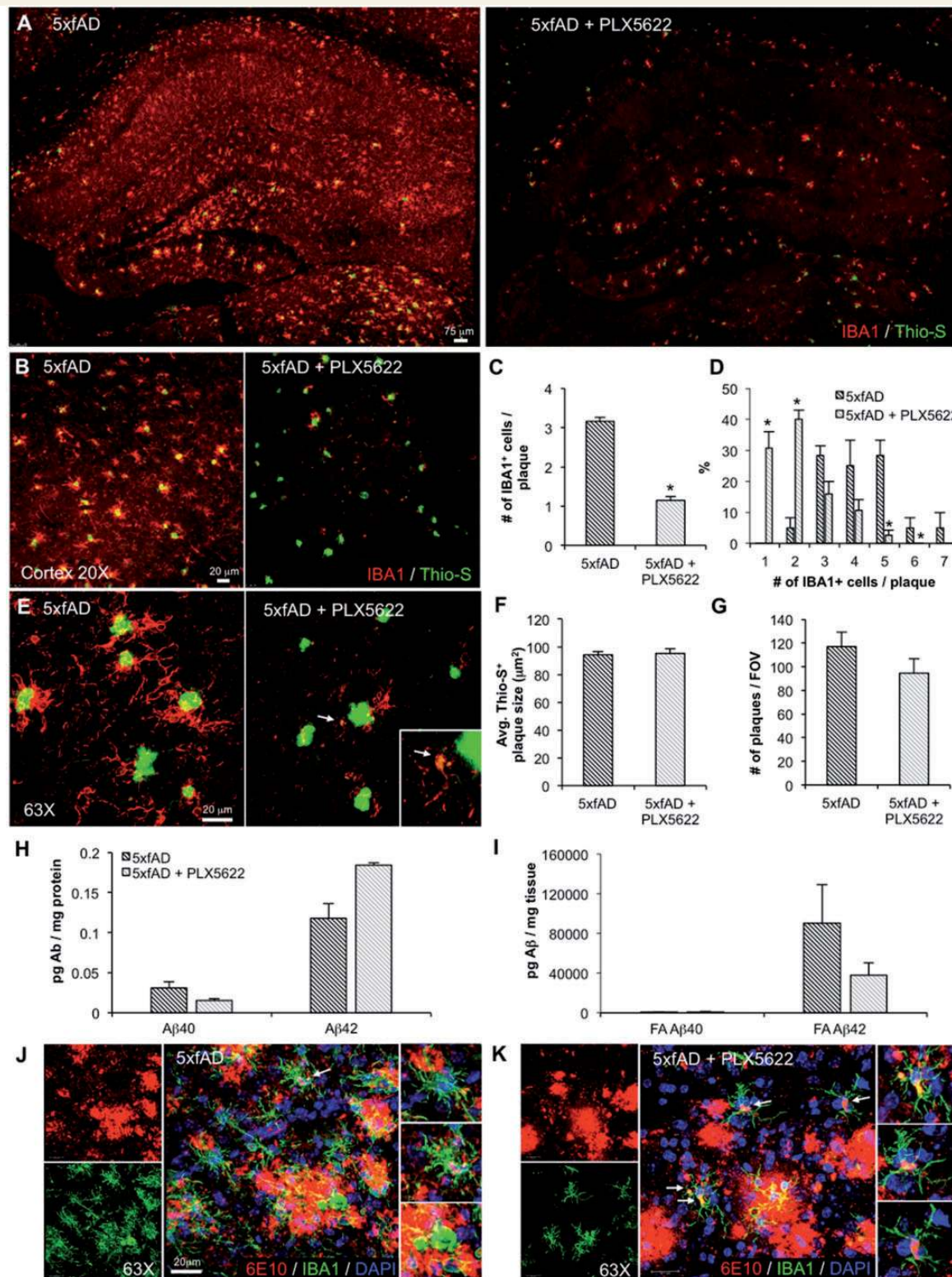
**Figure 5 Elimination of microglia with PLX5622.** Fourteen-month-old 5xfAD mice were treated with PLX5622 or control chow for 28 days. (**A, B** and **E**) Representative images showing dense-core plaques (Thio-S in green) and microglia (IBA1 in red) in the hippocampus and cortex. (**C** and **D**) Quantification reveals ~65% decrease in plaque-associated microglia with PLX5622 treatment (two-tailed unpaired *t*-test; $P < 0.0001$) and a significant increase in specifically 0 to 1 IBA1$^+$ cells associated with plaques in the PLX5622 group (two-tailed unpaired *t*-test; $P < 0.0001$). (**F** and **G**) Quantification of Thio-S$^+$ plaque areas and number of 6E10$^+$ plaques shows no effect of microglial elimination. (**H** and **I**) Levels of soluble and insoluble amyloid-β species in 5xfAD mice show no significant changes with microglial elimination. (**J** and **K**) 63X image of microglia (IBA1 in green), plaques (6E10 in red), and cell nuclei (DAPI in blue). Statistical significance is denoted by $^*P < 0.05$. Error bars indicate SEM ($n = 4$/group). FOV = field of view.

on average about one cell per plaque remaining (Fig. 5C); however, many plaques had no IBA1$^+$ cells associated with them (Fig. 5D). Further analyses revealed that all remaining IBA1$^+$ cells had cell bodies containing amyloid-β (Fig. 5K); in contrast, most IBA1$^+$ cells around plaques in untreated 5xfAD brains did not contain any amyloid-β (Fig. 5J). Indeed, some of these IBA1$^+$ cells in the treated mice were Thioflavin-S positive (Fig. 5E). However, as with the PLX3397-treated mice, we observed no change in the plaque area or total number (Fig. 5F and G), nor any significant changes in amyloid-β protein levels (Fig. 5H and I), with this cohort of microglia-eliminated 5xfAD mice.

## Alzheimer's disease-related gene transcription is altered in 5xfAD mice

RNA was extracted from flash-frozen brain tissue from 10-month-old mice treated with PLX3397 to analyse transcript levels of 180 inflammation-, Alzheimer's disease-, age-related genes, as part of a custom panel. Interestingly, transcript levels of *Apoe*, *Cstc*, and *Cstd*, which are implicated in lipid metabolism and protein degradation, respectively, were significantly increased in 5xfAD mice and attenuated with microglial elimination (Fig. 6A). No changes in *App*, *Bace1*, or ADAM10 mRNA were found with either genotype or treatment. Similarly, AD-related signalling is largely unaffected by microglial elimination. In accordance with mRNA data, western blot analysis of steady-state levels of APP showed no differences with treatment (Fig. 6B and C). Likewise, levels of the C-terminal fragments C99 and C83 showed no differences among groups (Fig. 6B and C).

## Microglial elimination reduces inflammation-related gene transcripts

As microglia are the primary immune cells of the brain, we wanted to determine how inflammatory signalling as a whole was impacted by microglial elimination in 5xfAD mice. RNA levels of many inflammation-related genes were significantly increased in 5xfAD mice compared to wild-type including complement (*C1qa*, *C4a*, and *C3*), chemokines (*Ccl12*, *Ccl3*, and *Ccl5*), and astrocytic genes (*Gfap* and S100). Crucially, the majority of increases are attenuated with microglial elimination in the 5xfAD mice (Fig. 7).

## Astrocyte numbers are largely unaffected with microglial elimination

As reactive gliosis is an important feature of Alzheimer's disease, we wanted to discern if microglial elimination impacts astrocyte numbers or responses. We immunolabelled tissue for reactive astrocytes using GFAP (green) and S100β (blue) with 6E10 (red) for plaques in the cortex and hippocampus (Supplementary Fig. 1A, B and D). GFAP

expression is restricted to the hippocampal area in wild-type mice, but is expressed in astrocytes around plaques in the cortex of 5xfAD mice, signifying reactive astrocytes. Accordingly, the number of GFAP$^+$ astrocytes was also increased in the hippocampal area, whilst S100β$^+$ astrocytes were also increased in both brain regions examined (Supplementary Fig. 1C). Notably, the number of GFAP$^+$ cells was reduced in the cortex of 5xfAD mice treated with PLX3397, while treatment did not affect GFAP$^+$ cells in the hippocampus, or S100β$^+$ cells in either brain region. We also probed for Aldh1L1$^+$ astrocytes—another marker of astrocyte reactivity. No Aldh1L1$^+$ cells were detected outside blood vessels in wild-type mice, but were apparent in 5xfAD animals where they were also GFAP$^+$ (Supplementary Fig. 1E–G). Quantification of Aldh1L1$^+$ astrocytes in hippocampus and cortex of 5xfAD mice showed no changes in expression with microglial elimination (Supplementary Fig. 1H).

## Microglial elimination restores dendritic spine number in 5xfAD mice

As activated microglia are thought to mediate synaptic stripping (Blinzinger and Kreutzberg, 1968; Wake et al., 2009), we sought to determine whether microglial elimination could affect dendritic spine number in 5xfAD mice. To that end, we stained tissue using the Golgi method (Fig. 8A) and counted and classified dendritic spines on non-primary apical dendrites in the CA1 region of the hippocampus (Fig. 8B and C). Total spine density was significantly decreased in 5xfAD mice compared to wild-type and a recovery of this effect was observed following microglial elimination (Fig. 8D). Specifically, mushroom spines were significantly decreased in the 5xfAD mice compared to controls, but the elimination of microglia significantly increased mushroom spines in 5xfAD mice. Elimination also shows a trend toward recovery of thin spines in these mice (Fig. 8D). Together, these data confirm previous findings of significant spine loss in the 5xfAD mouse model, and indicate that microglia modulate this process, as the elimination of these cells allows for the regeneration of previously lost dendritic spines.

## Elimination of microglia prevents neuronal loss in 5xfAD mice

An important and distinct feature of the 5xfAD mouse model is that these mice display overt neuronal loss in the subiculum at later stages (Eimer and Vassar, 2013). As we had eliminated microglia over this crucial period, we stained brain tissue with Cresyl violet to visualize cell nuclei and stereologically quantified the number of neurons in the subiculum (Fig. 8E). Quantification of neuronal populations revealed a significant decrease in neuronal number in the 5xfAD mice in the microglia-intact animals, whereas microglial elimination in 5xfAD mice prevented
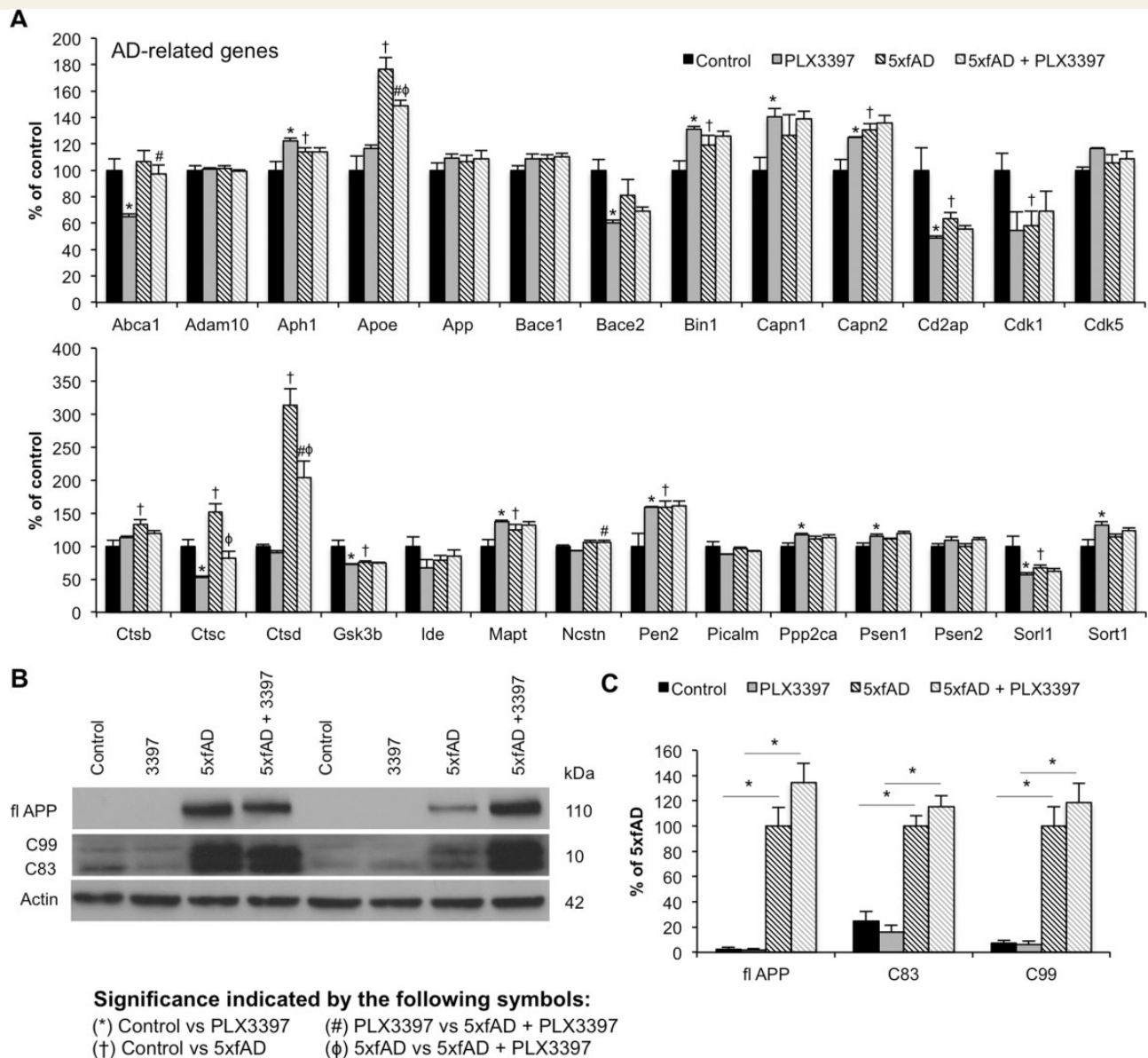
**Figure 6 Modest changes in Alzheimer's disease-related genes with microglial elimination.** Transcript levels for Alzheimer's disease-related genes were analysed using NanoString nCounter platform and immunoblots were performed to assess components of APP processing. (**A**) Alzheimer's disease-related gene transcript levels in all four experimental groups. Symbols denote significant differences between groups ($P < 0.05$): *Control versus PLX3397; †Control versus 5xfAD; #PLX3397 versus 5xfAD + PLX3397; φ5xfAD versus 5xfAD + PLX3397. (**B** and **C**) Immunoblotting for full-length APP, C99 and C83 showed significantly increased levels of each protein in 5xfAD mice compared to Control (via two-way ANOVA; $P < 0.0001$) and in 5xfAD + PLX3397 mice compared to PLX3397 (via two-way ANOVA; $P < 0.0001$), but showed no effect of microglial elimination in 5xfAD mice. Statistical significance is denoted by *$P < 0.05$. Error bars indicate SEM ($n = 3–6$/group).

this neuronal loss (Fig. 8F). These data corroborate previous reports of neuronal loss in the 5xfAD model in the subiculum at this age and indicate that microglia are actively contributing to neuronal loss in these mice.

# Discussion

The importance of microglia in Alzheimer's disease has been highlighted by genome-wide association studies, which have identified a number of single nucleotide polymorphisms (SNPs) associated with risk for the development of Alzheimer's disease that are associated with microglia function, including TREM2 (Guerreiro *et al.*, 2013), CD33 (Naj *et al.*, 2011), BIN1 (Seshadri *et al.*, 2010; Chapuis *et al.*, 2013), and CR1 (Lambert *et al.*, 2009). Thus, understanding the various roles that microglia play in the healthy and Alzheimer's disease brain are crucial to determine how these polymorphisms affect microglial function.
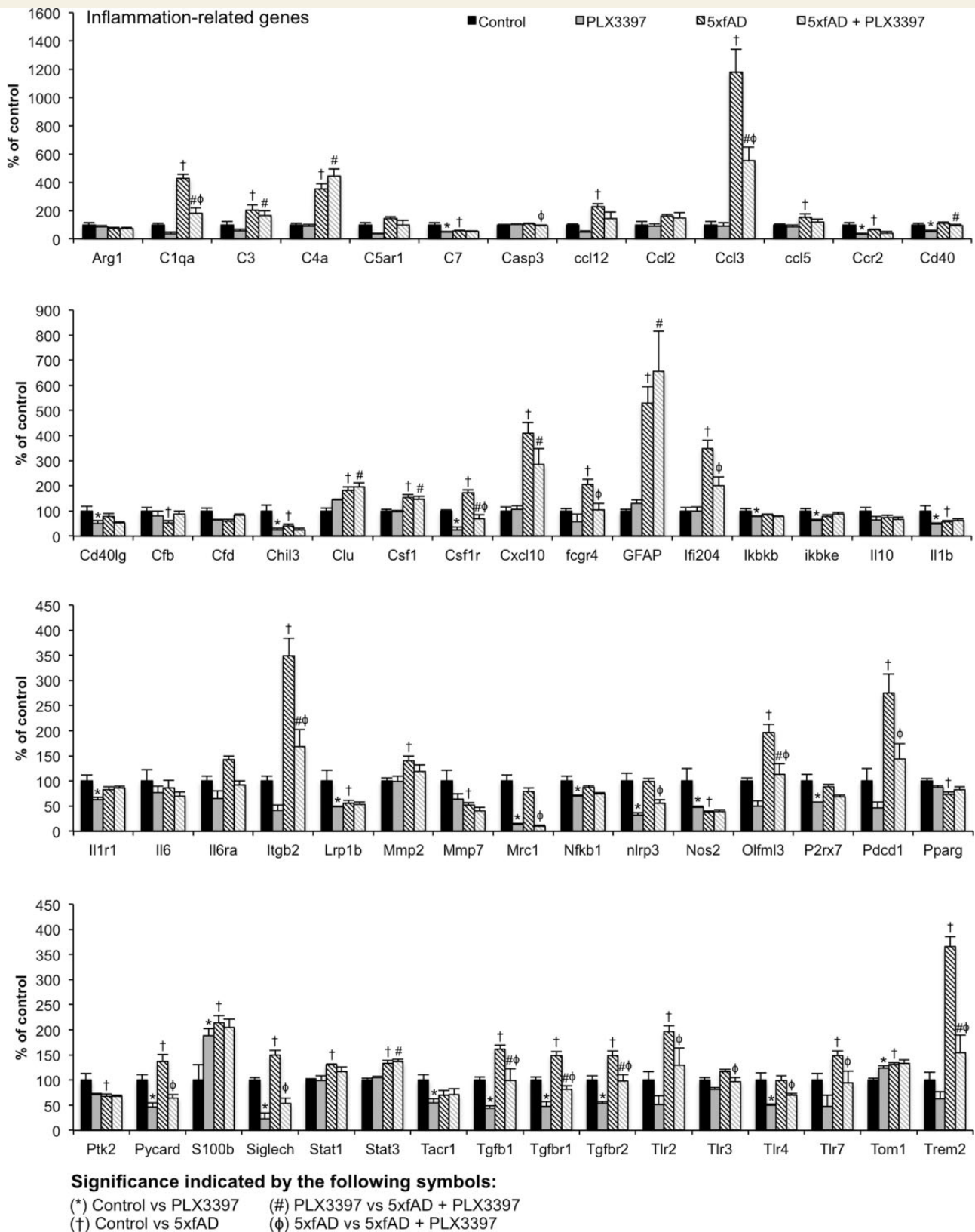
**Figure 7 Microglial elimination reduces neuroinflammatory signalling.** RNA transcripts for inflammation-related genes were analysed using NanoString nCounter platform. Symbols denote significant differences between groups ($P < 0.05$): symbols denote significant differences between groups ($P < 0.05$): *Control versus PLX3397; †Control versus 5xfAD; #PLX3397 versus 5xfAD + PLX3397; φ5xfAD versus 5xfAD + PLX3397. Error bars indicate SEM ($n$ = 3–6/group).

We have previously shown that microglial elimination can be achieved in the healthy adult mouse brain by treatment with small-molecule inhibitors of CSF1R (Elmore et al., 2014; Dagher et al., 2015), with many groups confirming our findings (Valdearcos et al., 2014; Asai et al., 2015; Klein et al., 2015; Schreiner et al., 2015). Here, we have extended these findings in mice constitutively expressing YFP under the Rosa26 locus in all CSF1R expressing cells to definitively show that microglia are eliminated and are not simply downregulating myeloid/microglial markers. We also found that chronically activated microglia following extensive neuronal injury can be eliminated with the same approach. Our studies also revealed that microglial elimination following neuronal insult improved functional outcomes, whereas elimination of microglia during the lesion exacerbated neuronal loss, revealing differential roles of microglia in injury response (Rice et al., 2015). It is important to note that only blood–brain barrier-permeant CSF1R inhibitors are able to eliminate microglia. These include the compounds PLX3397 and PLX5622 used in this study, as well as BLZ945 (Pyonteck et al., 2013). Furthermore, sustained brain exposure levels of CSF1R inhibitors are required for effective microglial elimination. It takes at least 3 days for microglia to succumb and die within the CNS (Elmore et al., 2014). It should be noted that CSF1R inhibitors are highly versatile; at high doses they eliminate microglia, allowing for the exploration into the roles of these cells in disease and normal brain function, while at lower doses they modulate CSF1R signalling in microglia without eliminating them. To this end, we have previously used low doses of PLX5622 (300 mg/kg chow rather than the 1200 mg/kg chow used in this study) to explore the role of the CSF1R in microglial response to Alzheimer's disease pathology and found that it regulates the chemotactic response of these cells to plaques (Dagher et al., 2015), resulting in improvements in cognition without affecting plaque burden or inflammatory profile. Moreover, the CSF1R has also been shown to be crucial for microglial proliferation during disease (Gomez-Nicola et al., 2013), also using CSF1R inhibitor paradigms that do not result in microglial elimination. In contrast, in this study, we sought to define the roles of microglia in mediating Alzheimer's disease pathogenesis through the administration of CSF1R inhibitors at doses sufficient to eliminate microglia, rather than at lower doses that modulate microglial function without eliminating them. We first set out to determine if microglia in the brains of aged 5xfAD mice are still dependent on CSF1R signalling for their survival. Importantly, we show that 28 days of continuous treatment with either PLX3397 or PLX5622 leads to an ~80–90% reduction in microglia, respectively, throughout the CNS in adult 5xfAD mice.

The elimination of microglia for 28 days from 5xfAD mice allows us to explore the role that these cells play in amyloid-β and plaque homeostasis/pathogenesis. Traditionally, it has been thought that microglia respond to the presence of amyloid-β plaques by helping clear them

from the brain via phagocytosis of amyloid-β-fibrils (Pan et al., 2011). Reactive microglia have been shown to encircle plaques and amyloid-β can be detected within their cytoplasm (Li et al., 2000; Webster et al., 2000; Koenigsknecht-Talboo and Landreth, 2005). Furthermore, a recent study showed that microglia tightly surround plaques and prevent further growth (Condello et al., 2015). However, results from a study of inducible microglial ablation found that eliminating microglia from the brains of APP overexpressing mice for 4 weeks does not affect plaque burden (Grathwohl et al., 2009). Our findings are in complete agreement with this, as we observed no changes in amyloid-β levels, either soluble or insoluble, following microglial elimination. Moreover, plaque load and average plaque size were also unaffected with CSF1R inhibitor treatment. Thus, microglia do not appear to affect brain amyloid-β levels and are not a source of significant amyloid-β clearance from the CNS, even in young, pre-pathological mice. Notably, we found a subset of CSF1R-inhibitor resistant IBA1⁺ cells following treatment and further analysis revealed that many of these cells associated with dense core plaques and contained amyloid-β within their cell bodies. The presence of these CSF1R-inhibitor resistant cells demonstrates heterogeneity of IBA1⁺ cells around plaques— even cells surrounding the same plaque may have different origins and functions. For example, recent studies that have crossed Trem2 knockout mice to App mice, including the 5xfAD model, have demonstrated a stark reduction in plaque-associated IBA1⁺ cells with Trem2 deletion. One study suggested that the reduction in these cells was due to a lack of infiltrating monocytes from the periphery (Jay et al., 2015)—as monocytes are not eliminated with the doses of CSF1R inhibitors used in this study (Chitu et al., 2012; Valdearcos et al., 2014)—this could also explain the subset of CSF1R-inhibitor resistant cells around plaques. Alternatively, TREM2 can act as a survival signal in place of CSF1R signalling (Wang et al., 2015), and it could be that a subset of IBA1⁺ cells around plaques upregulate Trem2, allowing them to survive in the presence of CSF1R inhibitors. As a parallel to our own findings, in a mouse model of glioblastoma multiforme with CSF1R inhibitor treatment, researchers found reduced numbers of tumour-associated IBA1⁺ cells, but not a complete eradication of these cells (Coniglio et al., 2012), providing further support of the existence of heterogeneous populations of IBA1⁺ cells in the brain. Regardless of the origin of the surviving IBA1⁺ cells, >30% of plaques in treated mice had no IBA1⁺ cells associated with them, and as we observed no effect on plaque number or size, these findings suggest that remaining IBA1⁺ cells are not significantly contributing to the regulation or maintenance of amyloid-β pathologies. Further evidence that microglia in the diseased brain are not protective against plaque development and growth has also come from studies with inducible APP transgenic mice, in which switching off the App transgene after plaque formation does not lead to the breakdown of plaques by the brain (Jankowsky et al., 2005).
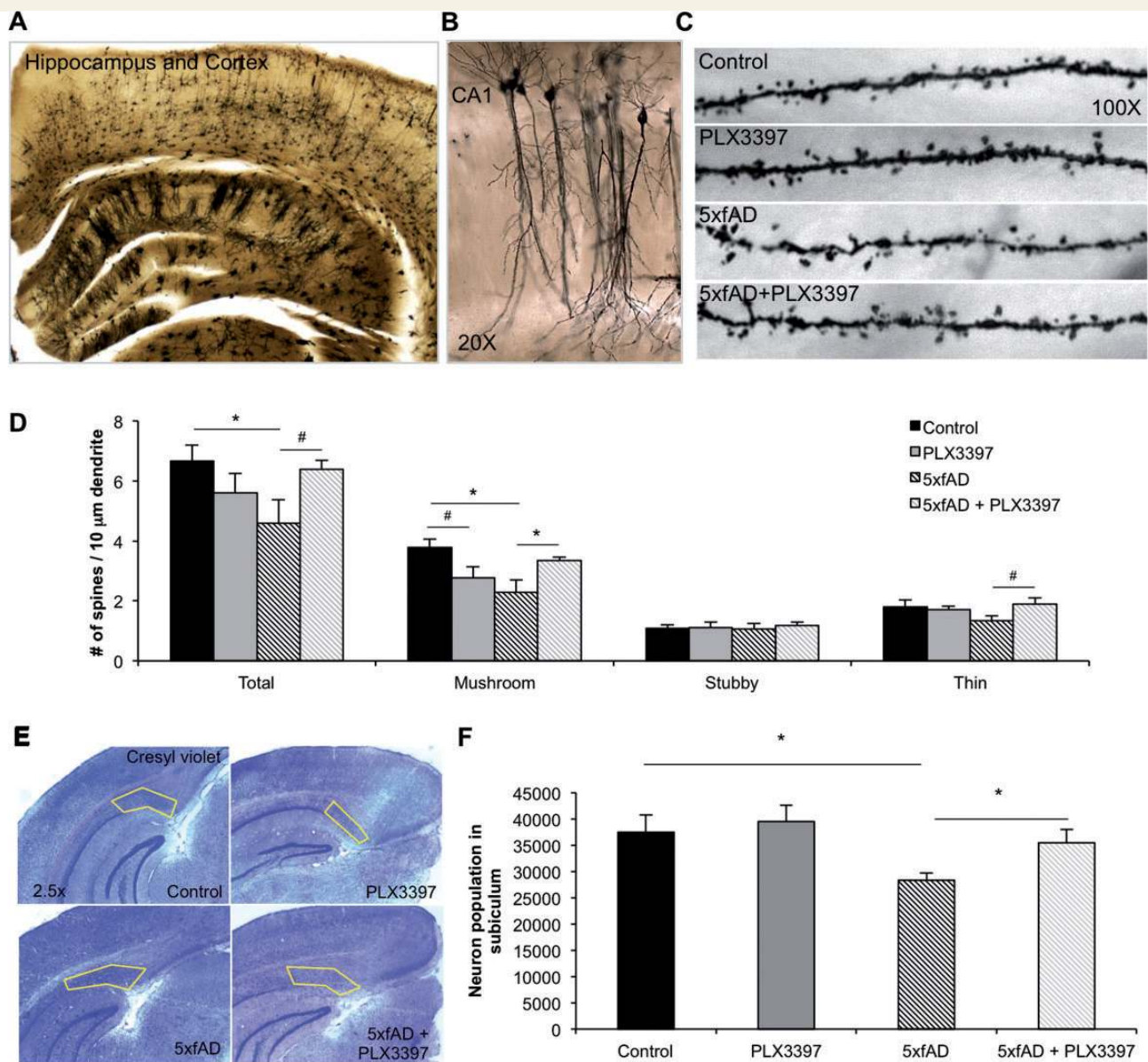
**Figure 8 Microglia modulate dendritic spine number in the CA1 and prevent neuronal loss in the subiculum of 5xfAD mice.** (**A**) Representative ×2.5 image of Golgi staining in hippocampus and cortex. (**B**) Representative ×20 image of CA1 neurons and dendritic branches. (**C**) Representative ×100 images of CA1 dendritic branches showing spines. (**D**) The number of total (two-way ANOVA; $P = 0.0337$) and mushroom (via two-way ANOVA; $P = 0.0091$) dendritic spines is significantly decreased in 5xfAD mice, compared to control. 5xfAD + PLX3397 mice show significantly increased mushroom spine density (via two-way ANOVA; $P = 0.0416$) and a trend for recovery of total spine loss (via two-way ANOVA; $P = 0.0561$), as well as a trend for increased thin spine density compared to 5xfAD (via two-way ANOVA; $P = 0.066$). (**E**) Representative ×2.5 images of Cresyl violet staining with the subiculum outlined in yellow. (**F**) Stereological quantification of the number of neurons in the 5xfAD group showed a significant decrease in cell number compared to control (two-way ANOVA; $P = 0.0181$). The neuronal loss in the 5xfAD group is prevented with microglial elimination in the 5xfAD + PLX3397 group (two-way ANOVA; $P = 0.0458$). Statistical significance is denoted by $^*P < 0.05$ and statistical trends by $^{\#}P < 0.10$. Error bars indicate SEM ($n = 3$–4/group).

Additionally, recent studies have shown that microglia around plaques are in a non-productive state due to over-production of IL10 (Chakrabarty et al., 2015), and that deletion of IL10 restimulates microglia to phagocytose and clear plaques (Guillot-Sestier et al., 2015). Similarly, it has been shown that prostaglandin E2 (PGE2) is over-produced in these conditions, and deletion of PGE2 stimulates the clearance of plaques (Johansson et al., 2015).

Likewise, studies using Alzheimer's disease mice on a Nos2 null background (to mimic the human system) show that microglia are suppressed around plaques and inhibitors of arginase can also restimulate these microglia to protect against Alzheimer's disease pathology (Kan et al., 2015). Following the findings that microglia in the presence of Alzheimer's disease pathology appear to be suppressed, stimulation of microglia is known to induce plaque

breakdown, with agents such as IL1β (Shaftel *et al.*, 2007), CSF1 (Boissonneault *et al.*, 2009), and lipopolysaccharide (DiCarlo *et al.*, 2001), as well as repeated scanning ultrasound treatments (Leinenga and Gotz, 2015). Collectively, these results are in agreement with our data and suggest that microglia in the Alzheimer's disease brain are not able to effectively clear amyloid-β from the CNS or protect against plaque formation or growth. Thus, given their chronic reactivity, it is imperative to determine what effects microglia are exerting in the Alzheimer's disease brain.

We found that elimination of microglia reduces brain-wide inflammatory signalling in 5xfAD mice, as indicated by RNA analysis of several inflammation-related genes. We observed reductions in microglia reactivity-associated transcripts, including *C1q*, *Tlr2*, *Tlr3*, *Tlr4*, *Tlr7*, *Ccl3*, *Nlrp3*, and *Pdcd1*, as well as reductions in anti-inflammatory/phagocytic markers, such as *Tgfb1*, *Tgfbr1*, *Tgfbr2*, *Mrc1*, and *Itgb2*. Additionally, our results show that elimination of microglia is beneficial for a hippocampal-dependent cognitive task. These findings are in line with many others that show modulating microglial function in Alzheimer's disease models can restore/improve memory (Kiyota *et al.*, 2010; Parachikova *et al.*, 2010; Gabbita *et al.*, 2012; Yamanaka *et al.*, 2012). Furthermore, others have shown that inflammatory factors are necessary for amyloid-β-induced long-term potentiation deficits (Costello *et al.*, 2015). Altogether, this suggests that microglia contribute to the memory impairments seen in Alzheimer's disease transgenic mice. Microglia produce a plethora of modulatory substances, but also interact with the local brain environment, and it is likely a combination of these activities that contributes to impairments. For example, *in vivo*, microglia have been shown to cause neuronal loss in Alzheimer's disease mice via signalling through CX3CR1, a chemokine receptor expressed by microglia involved in neuron-microglia communication (Fuhrmann *et al.*, 2010). Synaptic and neuronal loss is well documented in the 5xfAD model, and is likely one mechanism contributing to deficits in contextual memory (Jawhar *et al.*, 2012; Buskila *et al.*, 2013; Eimer and Vassar, 2013). In our study, we found the total number of dendritic spines to be significantly decreased in 5xfAD mice compared to controls, and this is accounted for primarily by decreases in mushroom spines. Critically, the elimination of microglia reversed reductions in mushroom spines in 5xfAD mice, suggesting that the absence of microglia allows for the regeneration of lost spines seen in the Alzheimer's disease brain. Additionally, we found a significant reduction of neurons in the subiculum of 5xfAD mice, which was prevented with the elimination of microglia, indicating an important and detrimental function of microglia in mediating neuronal loss in aged 5xfAD mice.

Overall, our results show that microglia in the diseased brain are dependent on CSF1R signalling for their survival. Importantly, we found that chronic microglial elimination is not detrimental to animals, but rather, improves functional outcomes and disease-related synaptic aberrations, while preventing neuronal loss.

# Acknowledgements

# Funding

# Supplementary material

Supplementary material is available at *Brain* online.

# References

Akama KT, Van Eldik LJ.Beta-amyloid stimulation of inducible nitric-oxide synthase in astrocytes is interleukin-1beta- and tumor necrosis factor-alpha (TNFalpha)-dependent, and involves a TNFalpha receptor-associated factor- and NFkappaB-inducing kinase-dependent signaling mechanism. J Biol Chem 2000; 275: 7918–24.

Akiyama H, Arai T, Kondo H, Tanno E, Haga C, Ikeda K. Cell mediators of inflammation in the Alzheimer disease brain. Alzheimer Dis Assoc Disord 2000; 14 (Suppl 1): S47–53.

Ando K, Brion JP, Stygelbout V, Suain V, Authelet M, Dedecker R, et al. Clathrin adaptor CALM/PICALM is associated with neurofibrillary tangles and is cleaved in Alzheimer's brains. Acta Neuropathol 2013; 125: 861–78.

Asai H, Ikezu S, Tsunoda S, Medalla M, Luebke J, Haydar T, et al. Depletion of microglia and inhibition of exosome synthesis halt tau propagation. Nat Neurosci 2015; 18: 1584–93.

Blinzinger K, Kreutzberg G. Displacement of synaptic terminals from regenerating motoneurons by microglial cells. Z Zellforsch Mikrosk Anat 1968; 85: 145–57.

Boissonneault V, Filali M, Lessard M, Relton J, Wong G, Rivest S. Powerful beneficial effects of macrophage colony-stimulating factor on beta-amyloid deposition and cognitive impairment in Alzheimer's disease. Brain 2009; 132 (Pt 4): 1078–92.

Bradshaw EM, Chibnik LB, Keenan BT, Ottoboni L, Raj T, Tang A, et al. CD33 Alzheimer's disease locus: altered monocyte function and amyloid biology. Nat Neurosci 2013; 16: 848–50.

Buskila Y, Crowe SE, Ellis-Davies GC. Synaptic deficits in layer 5 neurons precede overt structural decay in 5xFAD mice. Neuroscience 2013; 254: 152–9.

Butovsky O, Jedrychowski MP, Moore CS, Cialic R, Lanser AJ, Gabriely G, et al. Identification of a unique TGF-beta-dependent molecular and functional signature in microglia. Nat Neurosci 2014; 17: 131–43.

Cacquevel M, Lebeurrier N, Cheenne S, Vivien D. Cytokines in neuroinflammation and Alzheimer's disease. Curr Drug Targets 2004; 5: 529–34.

Cagnin A, Brooks DJ, Kennedy AM, Gunn RN, Myers R, Turkheimer FE, et al. In-vivo measurement of activated microglia in dementia. Lancet 2001; 358: 461–7.

Centonze D, Muzio L, Rossi S, Cavasinni F, De Chiara V, Bergami A, et al. Inflammation triggers synaptic alteration and degeneration in experimental autoimmune encephalomyelitis. J Neurosci 2009; 29: 3442–52.

Chakrabarty P, Li A, Ceballos-Diaz C, Eddy JA, Funk CC, Moore B, et al. IL-10 alters immunoproteostasis in APP mice, increasing plaque burden and worsening cognitive behavior. Neuron 2015; 85: 519–33.

Chapuis J, Hansmannel F, Gistelinck M, Mounier A, Van Cauwenberghe C, Kolen KV, et al. Increased expression of BIN1 mediates Alzheimer genetic risk by modulating tau pathology. Mol Psychiatry 2013; 18: 1225–34.

Chitu V, Nacu V, Charles JF, Henne WM, McMahon HT, Nandi S, et al. PSTPIP2 deficiency in mice causes osteopenia and increased differentiation of multipotent myeloid precursors into osteoclasts. Blood 2012; 120: 3126–35.

Condello C, Yuan P, Schain A, Grutzendler J. Microglia constitute a barrier that prevents neurotoxic protofibrillar Abeta42 hotspots around plaques. Nat Commun 2015; 6: 6176.

Coniglio SJ, Eugenin E, Dobrenis K, Stanley ER, West BL, Symons MH, et al. Microglial stimulation of glioblastoma invasion involves epidermal growth factor receptor (EGFR) and colony stimulating factor 1 receptor (CSF-1R) signaling. Mol Med 2012; 18: 519–27.

Costello DA, Carney DG, Lynch MA. alpha-TLR2 antibody attenuates the Abeta-mediated inflammatory response in microglia through enhanced expression of SIGIRR. Brain Behav Immun 2015; 46: 70–9.

Crehan H, Hardy J, Pocock J. Blockage of CR1 prevents activation of rodent microglia. Neurobiol Dis 2013; 54: 139–49.

Crowe SE, Ellis-Davies GC. Spine pruning in 5xFAD mice starts on basal dendrites of layer 5 pyramidal neurons. Brain Struct Funct 2014; 219: 571–80.

Dagher NN, Najafi AR, Kayala KM, Elmore MR, White TE, Medeiros R, et al. Colony-stimulating factor 1 receptor inhibition prevents microglial plaque association and improves cognition in 3xTg-AD mice. J Neuroinflammation 2015; 12: 139.

Dandrea MR, Reiser PA, Gumula NA, Hertzog BM, Andrade-Gordon P. Application of triple immunohistochemistry to characterize amyloid plaque-associated inflammation in brains with Alzheimer's disease. Biotech Histochem 2001; 76: 97–106.

DiCarlo G, Wilcock D, Henderson D, Gordon M, Morgan D. Intrahippocampal LPS injections reduce Abeta load in APP + PS1 transgenic mice. Neurobiol Aging 2001; 22: 1007–12.

Dickson DW, Farlo J, Davies P, Crystal H, Fuld P, Yen SH. Alzheimer's disease: a double-labeling immunohistochemical study of senile plaques. Am J Pathol 1988; 132: 86–101.

Dong H, Martin MV, Chambers S, Csernansky JG. Spatial relationship between synapse loss and beta-amyloid deposition in Tg2576 mice. J Comp Neurol 2007; 500: 311–21.

Eimer WA, Vassar R. Neuron loss in the 5XFAD mouse model of Alzheimer's disease correlates with intraneuronal Abeta42 accumulation and Caspase-3 activation. Mol Neurodegener 2013; 8: 2.

Elmore MR, Lee RJ, West BL, Green KN. Characterizing newly repopulated microglia in the adult mouse: impacts on animal behavior, cell morphology, and neuroinflammation. PLoS One 2015; 10: e0122912.

Elmore MR, Najafi AR, Koike MA, Dagher NN, Spangenberg EE, Rice RA, et al. Colony-stimulating factor 1 receptor signaling is necessary for microglia viability, unmasking a microglia progenitor cell in the adult brain. Neuron 2014; 82: 380–97.

Fillit H, Ding WH, Buee L, Kalman J, Altstiel L, Lawlor B, et al. Elevated circulating tumor necrosis factor levels in Alzheimer's disease. Neurosci Lett 1991; 129: 318–20.

Fuhrmann M, Bittner T, Jung CK, Burgold S, Page RM, Mitteregger G, et al. Microglial Cx3cr1 knockout prevents neuron loss in a mouse model of Alzheimer's disease. Nat Neurosci 2010; 13: 411–13.

Gabbita SP, Srivastava MK, Eslami P, Johnson MF, Kobritz NK, Tweedie D, et al. Early intervention with a small molecule inhibitor for tumor necrosis factor-alpha prevents cognitive deficits in a triple transgenic mouse model of Alzheimer's disease. J Neuroinflammation 2012; 9: 99.

Gomez-Nicola D, Fransen NL, Suzzi S, Perry VH. Regulation of microglial proliferation during chronic neurodegeneration. J Neurosci 2013; 33: 2481–93.

Grathwohl SA, Kalin RE, Bolmont T, Prokop S, Winkelmann G, Kaeser SA, et al. Formation and maintenance of Alzheimer's disease beta-amyloid plaques in the absence of microglia. Nat Neurosci 2009; 12: 1361–3.

Grutzendler J, Gan WB. Long-term two-photon transcranial imaging of synaptic structures in the living brain. CSH Protoc 2007; 2007: pdb prot4766.

Guerreiro R, Wojtas A, Bras J, Carrasquillo M, Rogaeva E, Majounie E, et al. TREM2 variants in Alzheimer's disease. N Engl J Med 2013; 368: 117–27.

Guillot-Sestier MV, Doty KR, Gate D, Rodriguez J Jr, Leung BP, Rezai-Zadeh K, et al. Il10 deficiency rebalances innate immunity to mitigate Alzheimer-like pathology. Neuron 2015; 85: 534–48.

Hauss-Wegrzyniak B, Lynch MA, Vraniak PD, Wenk GL. Chronic brain inflammation results in cell loss in the entorhinal cortex and impaired LTP in perforant path-granule cell synapses. Exp Neurol 2002; 176: 336–41.

Ishizuka K, Kimura T, Igata-yi R, Katsuragi S, Takamatsu J, Miyakawa T. Identification of monocyte chemoattractant protein-1 in senile plaques and reactive microglia of Alzheimer's disease. Psychiatry Clin Neurosci 1997; 51: 135–8.

Jankowsky JL, Slunt HH, Gonzales V, Savonenko AV, Wen JC, Jenkins NA, et al. Persistent amyloidosis following suppression of Abeta production in a transgenic model of Alzheimer disease. PLoS Med 2005; 2: e355.

Jawhar S, Trawicka A, Jenneckens C, Bayer TA, Wirths O. Motor deficits, neuron loss, and reduced anxiety coinciding with axonal degeneration and intraneuronal Abeta aggregation in the 5XFAD mouse model of Alzheimer's disease. Neurobiol Aging 2012; 33: 196.e29–40.

Jay TR, Miller CM, Cheng PJ, Graham LC, Bemiller S, Broihier ML, et al. TREM2 deficiency eliminates TREM2 + inflammatory macrophages and ameliorates pathology in Alzheimer's disease mouse models. J Exp Med 2015; 212: 287–95.

Johansson JU, Woodling NS, Wang Q, Panchal M, Liang X, Trueba-Saiz A, et al. Prostaglandin signaling suppresses beneficial microglial function in Alzheimer's disease models. J Clin Invest 2015; 125: 350–64.

Kan MJ, Lee JE, Wilson JG, Everhart AL, Brown CM, Hoofnagle AN, et al. Arginine deprivation and immune suppression in a mouse model of Alzheimer's disease. J Neurosci 2015; 35: 5969–82.

Kim TS, Cavnar MJ, Cohen NA, Sorenson EC, Greer JB, Seifert AM, et al. Increased KIT inhibition enhances therapeutic efficacy in gastrointestinal stromal tumor. Clin Cancer Res 2014; 20: 2350–62.

Kim WS, Li H, Ruberu K, Chan S, Elliott DA, Low JK, et al. Deletion of Abca7 increases cerebral amyloid-beta accumulation in the J20 mouse model of Alzheimer's disease. J Neurosci 2013; 33: 4387–94.

Kitazawa M, Cheng D, Tsukamoto MR, Koike MA, Wes PD, Vasilevko V, et al. Blocking IL-1 signaling rescues cognition, attenuates tau pathology, and restores neuronal beta-catenin pathway function in an Alzheimer's disease model. J Immunol 2011; 187: 6539–49.

Kitazawa M, Oddo S, Yamasaki TR, Green KN, LaFerla FM. Lipopolysaccharide-induced inflammation exacerbates tau pathology

by a cyclin-dependent kinase 5-mediated pathway in a transgenic model of Alzheimer's disease. J Neurosci 2005; 25: 8843–53.

Kiyota T, Okuyama S, Swan RJ, Jacobsen MT, Gendelman HE, Ikezu T. CNS expression of anti-inflammatory cytokine interleukin-4 attenuates Alzheimer's disease-like pathogenesis in APP + PS1 bigenic mice. FASEB J 2010; 24: 3093–102.

Klein D, Patzko A, Schreiber D, van Hauwermeiren A, Baier M, Groh J, et al. Targeting the colony stimulating factor 1 receptor alleviates two forms of Charcot-Marie-Tooth disease in mice. Brain 2015; 138 (Pt 11): 3193–205.

Koenigsknecht-Talboo J, Landreth GE. Microglial phagocytosis induced by fibrillar beta-amyloid and IgGs are differentially regulated by proinflammatory cytokines. J Neurosci 2005; 25: 8240–9.

Lambert JC, Heath S, Even G, Campion D, Sleegers K, Hiltunen M, et al. Genome-wide association study identifies variants at CLU and CR1 associated with Alzheimer's disease. Nat Genet 2009; 41: 1094–9.

Leinenga G, Gotz J. Scanning ultrasound removes amyloid-beta and restores memory in an Alzheimer's disease mouse model. Sci Transl Med 2015; 7: 278ra33.

Li R, Shen Y, Yang LB, Lue LF, Finch C, Rogers J. Estrogen enhances uptake of amyloid beta-protein by microglia derived from the human cortex. J Neurochem 2000; 75: 1447–54.

Mattiace LA, Davies P, Yen SH, Dickson DW. Microglia in cerebellar plaques in Alzheimer's disease. Acta Neuropathol 1990; 80: 493–8.

McGeer EG, McGeer PL. Brain inflammation in Alzheimer disease and the therapeutic implications. Curr Pharm Des 1999; 5: 821–36.

Meda L, Cassatella MA, Szendrei GI, Otvos L Jr, Baron P, Villalba M, et al. Activation of microglial cells by beta-amyloid protein and interferon-gamma. Nature 1995; 374: 647–50.

Medway C, Morgan K. Review: The genetics of Alzheimer's disease; putting flesh on the bones. Neuropathol Appl Neurobiol 2014; 40: 97–105.

Mok S, Koya RC, Tsui C, Xu J, Robert L, Wu L, et al. Inhibition of CSF1 receptor improves the anti-tumor efficacy of adoptive cell transfer immunotherapy. Cancer Res 2014; 74: 153–61.

Myczek K, Yeung ST, Castello N, Baglietto-Vargas D, LaFerla FM. Hippocampal adaptive response following extensive neuronal loss in an inducible transgenic mouse model. PLoS One 2014; 9: e106009

Naj AC, Jun G, Beecham GW, Wang LS, Vardarajan BN, Buros J, et al. Common variants at MS4A4/MS4A6E, CD2AP, CD33 and EPHA1 are associated with late-onset Alzheimer's disease. Nat Genet 2011; 43: 436–41.

Neely KM, Green KN, LaFerla FM. Presenilin is necessary for efficient proteolysis through the autophagy-lysosome system in a gamma-secretase-independent manner. J Neurosci 2011; 31: 2781–91.

Oakley H, Cole SL, Logan S, Maus E, Shao P, Craft J, et al. Intraneuronal beta-amyloid aggregates, neurodegeneration, and neuron loss in transgenic mice with five familial Alzheimer's disease mutations: potential factors in amyloid plaque formation. J Neurosci 2006; 26: 10129–40.

Pan XD, Zhu YG, Lin N, Zhang J, Ye QY, Huang HP, et al. Microglial phagocytosis induced by fibrillar beta-amyloid is attenuated by oligomeric beta-amyloid: implications for Alzheimer's disease. Mol Neurodegener 2011; 6: 45.

Parachikova A, Vasilevko V, Cribbs DH, LaFerla FM, Green KN. Reductions in amyloid-beta-derived neuroinflammation, with minocycline, restore cognition but do not significantly affect tau hyperphosphorylation. J Alzheimers Dis 2010; 21: 527–42.

Peters A, Kaiserman-Abramof IR. The small pyramidal neuron of the rat cerebral cortex: the perikaryon, dendrites and spines. Am J Anat 1970; 127: 321–55.

Pyonteck SM, Akkari L, Schuhmacher AJ, Bowman RL, Sevenich L, Quail DF, et al. CSF-1R inhibition alters macrophage polarization and blocks glioma progression. Nat Med 2013; 19: 1264–72.

Rice RA, Berchtold NC, Cotman CW, Green KN. Age-related downregulation of the CaV3.1 T-type calcium channel as a mediator of amyloid beta production. Neurobiol Aging 2014; 35: 1002–11.

Rice RA, Spangenberg EE, Yamate-Morgan H, Lee RJ, Arora RP, Hernandez MX, et al. Elimination of microglia improves functional outcomes following extensive neuronal loss in the hippocampus. J Neurosci 2015; 35: 9977–89.

Robinson JL, Molina-Porcel L, Corrada MM, Raible K, Lee EB, Lee VM, et al. Perforant path synaptic loss correlates with cognitive impairment and Alzheimer's disease in the oldest-old. Brain 2014; 137 (Pt 9): 2578–87.

Rodriguez-Ortiz CJ, Hoshino H, Cheng D, Liu-Yescevitz L, Blurton-Jones M, Wolozin B, et al. Neuronal-specific overexpression of a mutant valosin-containing protein associated with IBMPFD promotes aberrant ubiquitin and TDP-43 accumulation and cognitive dysfunction in transgenic mice. Am J Pathol 2013; 183: 504–15.

Rozemuller JM, Eikelenboom P, Stam FC. Role of microglia in plaque formation in senile dementia of the Alzheimer type. An Immunohistochemical Study Virchows Arch B Cell Pathol Incl Mol Pathol 1986; 51: 247–54.

Scheff SW, Price DA, Schmitt FA, Mufson EJ. Hippocampal synaptic loss in early Alzheimer's disease and mild cognitive impairment. Neurobiol Aging 2006; 27: 1372–84.

Schreiner B, Romanelli E, Liberski P, Ingold-Heppner B, Sobottka-Brillout B, Hartwig T, et al. Astrocyte Depletion Impairs Redox Homeostasis and Triggers Neuronal Loss in the Adult CNS. Cell Rep 2015; 12: 1377–84.

Seshadri S, Fitzpatrick AL, Ikram MA, DeStefano AL, Gudnason V, Boada M, et al. Genome-wide analysis of genetic loci associated with Alzheimer disease. JAMA 2010; 303: 1832–40.

Shaftel SS, Kyrkanides S, Olschowka JA, Miller JN, Johnson RE, O'Banion MK. Sustained hippocampal IL-1 beta overexpression mediates chronic neuroinflammation and ameliorates Alzheimer plaque pathology. J Clin Invest 2007; 117: 1595–604.

Spires-Jones TL, Meyer-Luehmann M, Osetek JD, Jones PB, Stern EA, Bacskai BJ, et al. Impaired spine stability underlies plaque-related spine loss in an Alzheimer's disease mouse model. Am J Pathol 2007; 171: 1304–11.

Srivatsan S, Swiecki M, Otero K, Cella M, Shaw AS. CD2-associated protein regulates plasmacytoid dendritic cell migration, but is dispensable for their development and cytokine production. J Immunol 2013; 191: 5933–40.

Tap WD, Wainberg ZA, Anthony SP, Ibrahim PN, Zhang C, Healey JH, et al. Structure-guided blockade of CSF1R kinase in tenosynovial giant-cell tumor. N Engl J Med 2015; 373: 428–37.

Valdearcos M, Robblee MM, Benjamin DI, Nomura DK, Xu AW, Koliwad SK. Microglia dictate the impact of saturated fat consumption on hypothalamic inflammation and neuronal function. Cell Rep 2014; 9: 2124–38.

Wake H, Moorhouse AJ, Jinno S, Kohsaka S, Nabekura J. Resting microglia directly monitor the functional state of synapses in vivo and determine the fate of ischemic terminals. J Neurosci 2009; 29: 3974–80.

Wang Y, Cella M, Mallinson K, Ulrich JD, Young KL, Robinette ML, et al. TREM2 lipid sensing sustains the microglial response in an Alzheimer's disease model. Cell 2015; 160: 1061–71.

Webster SD, Yang AJ, Margol L, Garzon-Rodriguez W, Glabe CG, Tenner AJ. Complement component C1q modulates the phagocytosis of Abeta by microglia. Exp Neurol 2000; 161: 127–38.

Xu Q, Li Y, Cyras C, Sanan DA, Cordell B. Isolation and characterization of apolipoproteins from murine microglia. Identification of a low density lipoprotein-like apolipoprotein J-rich but E-poor spherical particle. J Biol Chem 2000; 275: 31770–7.

Yamanaka M, Ishikawa T, Griep A, Axt D, Kummer MP, Heneka MT. PPARgamma/RXRalpha-induced and CD36-mediated microglial amyloid-beta phagocytosis results in cognitive improvement in amyloid precursor protein/presenilin 1 mice. J Neurosci 2012; 32: 17321–31.

Ziehn MO, Avedisian AA, Tiwari-Woodruff S, Voskuhl RR. Hippocampal CA1 atrophy and synaptic loss during experimental autoimmune encephalomyelitis, EAE. Lab Invest 2010; 90: 774–86.